

High-throughput screening and interpretable machine learning model of
single-atom hydrogen evolution catalysts with asymmetric coordination
environment constructed by heteroatom-doped graphdiyne

Ying Zhao^{a*†}; Shuai-Shuai Gao^{a†}; Hui-Peng Ren ^a; Li-Shuang Ma ^b; Xue-Bo Chen ^{a,c*}

^a Shandong Laboratory of Advanced Materials and green Manufacturing at Yantai, Yantai
264000, P. R. China.

^b College of Chemistry and Chemical Engineering, State Key Laboratory of Heavy Oil

^c College of Chemistry, Beijing Normal University, Beijing, 100091, P. R. China

* Corresponding author email: yingz@amgm.ac.cn; xuebochen@bnu.edu.cn

† These authors contributed equally to this work and should be considered co-first authors

Table. S1 The formation energies (E_f) of HM@NM–GDY in units of eV

HM-GDY	E_f
N1	-7.3880
N2	-8.2008
B1	-4.3552
B2	-5.3473
S1	-4.1468
S2	-4.3388
B1S2	-3.4610
B1S3	-7.3080
B1S4	-9.6610
B2S1	-3.7872
B2S3	-9.9717
B2S4	-10.7098
N1B2	-8.0363
N1B3	-10.5460
N1B4	-13.4920
N2B1	-7.7678
N2B3	-12.9711
N2B4	-14.1752
N1S2	-6.2693
N1S3	-9.9797
N1S4	-12.5373
N2S1	-6.1456
N2S3	-12.5050
N2S4	-13.1408

Table. S2 The formation energies (E_f) of the 120 kinds of TM@NM–GDY in units of eV. The number of coordination between the metal atom and the environment atoms.

E_f	Cr		Mn		Fe		Co		Ni	
N1	-6.1275	4	-5.7635	4	-5.9639	4	-5.9644	4	-6.0676	4
N2	-6.7572	4	-6.8480	4	-7.0861	4	-7.0009	4	-7.1457	4
B1	-3.5791	4	-4.2918	4	-4.2345	4	-3.8934	4	-4.3814	4
B2	2.0810	4	-5.4276	4	-5.3001	4	-4.9144	4	-5.2794	4
S1	-3.7744	4	-3.8208	4	-4.0237	4	-3.8211	4	-3.7770	4
S2	-3.3384	4	-4.7402	4	-4.8800	4	-4.6050	4	-4.7376	4
B1S2	-2.1643	5	-1.6973	6	-2.0514	6	-3.3618	4	-3.3894	4
B1S3	-6.6830	5	-6.9492	5	-6.9490	4	-6.6332	4	-6.8236	4
B1S4	-	-	-	-	-	-	-10.6203	5	-	-
B2S1	-2.8308	5	-	-	-3.8229	4	-3.7175	4	-3.6128	4
B2S3	-9.1953	4	-9.7236	5	-9.6978	4	-9.3476	4	-9.5812	4
B2S4	-10.7773	4	-11.3748	5	-11.4245	4	-11.1294	4	-11.2373	4
N1B2	-6.0188	4	-6.1945	4	-5.5637	4	-6.0787	4	-6.7106	4

N1B3	-9.8209	4	-9.8381	4	-9.3262	4	-9.6993	4	-10.1160	4
N1B4	-	-	-12.8893	4	-12.7883	4	-12.5181	4	-12.9821	4
N2B1	-5.6646	5	-6.2123	4	-6.2632	4	-6.2583	4	-6.6833	4
N2B3	-12.7578	4	-11.3435	5	-12.4909	4	-12.7426	4	-12.9182	4
N2B4	-	-	-13.7497	4	-13.7896	4	-13.6124	4	-13.9246	4
N1S2	-5.0721	4	-4.9817	4	-4.7393	4	-	-	-	-
N1S3	-6.5657	4	-6.8314	4	-7.5857	4	-7.8219	4	-8.1475	4
N1S4	-11.1308	5	-	-	-10.1793	4	-10.6378	4	-10.9456	4
N2S1	-	-	-	-	-	-	-	-	-	-
N2S3	-11.1998	4	-11.0008	4	-11.0652	4	-11.1719	4	-11.3498	4
N2S4	-12.0154	4	-	-	-11.7387	4	-11.8070	4	-12.0309	4

Table. S3 The adsorption energies (E_{ads}) of the 103 kinds of TM@NM–GDY in units of eV and the bond lengths in units of Å.

E_f	Cr		Mn		Fe		Co		Ni	
	E_{ads}	$d_{\text{TM-H}}$	E_{ads}	$d_{\text{TM-H}}$	E_{ads}	$d_{\text{TM-H}}$	E_{ads}	$d_{\text{TM-H}}$	E_{ads}	$d_{\text{TM-H}}$
N1	0.5685	1.591	0.1575	1.538	-0.1415	1.475	0.2254	1.476	-0.3918	1.48
N2	0.1978	1.59	0.1499	1.535	-0.0036	1.479	-0.8072	1.447	-0.2860	1.484
B1	0.1942	1.603	0.2785	1.563	0.1576	1.498	-0.2054	1.465	0.2382	1.445
B2	-	-	0.2404	1.581	0.1253	1.496	-0.6166	1.588	-0.5054	1.561
S1	-0.1285	1.612	-0.0499	1.556	-0.0630	1.533	0.2795	1.494	-0.1345	1.482
S2	-0.9787	1.6	0.0825	1.555	0.1335	1.518	0.0216	1.475	0.3051	1.523
B1S2	-0.4035	1.58	-0.0245	1.576	-	-	0.1867	1.464	0.2433	1.523
B1S3	-0.0044	1.584	-0.1107	1.589	-0.1215	1.561	-0.0576	1.525	-0.0248	1.500
B1S4	-	-	-	-	-	-	0.0313	1.459	-	-
B2S1	-1.1400	1.752	-	-	-0.1063	1.524	-0.5470	1.694	-0.9780	1.656
B2S3	-0.2294	1.59	0.3391	1.545	0.0981	1.509	0.0596	1.464	-0.0453	1.502
B2S4	-0.2049	1.584	0.1923	1.567	-0.0140	1.513	0.0584	1.462	-1.0092	1.622
N1B2	0.1261	1.593	-0.1305	1.600	-0.5536	1.482	-0.1642	1.445	0.0432	1.598
N1B3	0.1353	1.604	-0.0043	1.61	-0.5758	1.493	-0.1844	1.449	0.5892	1.486
N1B4	-	-	0.2716	1.547	0.0115	1.488	-0.2451	1.452	0.1069	1.542
N2B1	-0.2423	1.591	0.5820	1.535	0.0028	1.490	0.0529	1.443	0.8029	1.518
N2B3	0.2199	1.595	-	-	-0.5457	1.490	-0.0592	1.452	0.1940	1.499
N2B4	-	-	0.2806	1.535	0.0237	1.491	-0.0304	1.444	0.1705	1.497
N1S2	-0.0740	1.6	0.1472	1.540	-0.3066	1.488	-	-	-	-
N1S3	-1.7939	1.633	-1.3506	1.599	-0.2774	1.485	-0.1492	1.506	-	-
N1S4	0.0393	1.614	-	-	-0.3396	1.511	0.0460	1.487	0.4258	1.48
N2S1	-	-	-	-	-	-	-	-	-	-
N2S3	0.2347	1.594	0.0477	1.605	-0.1229	1.48	0.0261	1.463	-0.0114	1.491
N2S4	0.2416	1.595	-	-	-0.1038	1.481	-0.0010	1.458	0.2892	1.474

Table S4 The obtained Gibbs free energy of adsorption of hydrogen (ΔG_{*H}) for TM@NM-GDY.

	Cr	Mn	Fe	Co	Ni
N1	0.8121	0.4181	0.1284	0.4627	-0.1400
N2	0.4407	0.4192	0.2274	-0.5240	-0.0209
B1	0.3898	0.5161	0.4148	0.0622	0.4958
B2	-	0.4548	0.3705	-0.3177	-0.1984
S1	0.1074	0.2062	0.1752	0.5480	0.1092
S2	-0.7555	0.2846	0.3946	0.2989	0.5387
B1S2	-0.1444	0.2125	-	0.4557	0.4920
B1S3	0.2491	0.1073	0.1152	0.1800	0.2343
B1S4	-	-	-	0.2860	-
B2S1	-0.8393	-	0.1533	-0.2547	-0.6799
B2S3	0.0097	0.5924	0.3218	0.3119	0.2114
B2S4	0.0437	0.4516	0.2430	0.3261	-0.6876
N1B2	0.3605	0.0467	-0.3044	0.1126	0.3433
N1B3	0.3257	0.1782	-0.3259	0.0857	0.8260
N1B4	-	0.5233	0.2749	0.0353	0.3946
N2B1	-0.0046	0.8486	0.2520	0.3401	1.0373
N2B3	0.4610	-0.8521	-0.2694	0.2160	0.4477
N2B4	-	0.5323	0.2909	0.2503	0.4115
N1S2	0.1768	0.3544	-0.0356	-	-
N1S3	-1.5762	-1.1193	-0.0189	0.1076	-0.9670
N1S4	0.2626	-	-0.0847	0.3075	0.6846
N2S1	-	-	-	-	-
N2S3	0.4616	0.2775	0.1358	0.3039	0.2399
N2S4	0.4677	-	0.1778	0.2737	0.5332

Table S5 The adsorption energies (E_{ads}) of the possible TM adsorption sites for five potential HER catalysts in units of eV.

	Cr@N2B1- GDY	Mn@N1B2- GDY	Fe@N1S2- GDY	Co@N1B4- GDY	Ni@N2- GDY
1	-4.83	-	-	-	-6.06
2	-4.45	-5.08	-	-	-6.06
3	-2.35	-5.03	-	-11.45	-5.67
4	-5.66	-6.19	-4.74	-12.52	-7.15

Table S6 The adsorption free energies (ΔG_{*H}) of different adsorption sites in the five candidates.

SACs	$\Delta G_{*H}(N)$	$\Delta G_{*H}(B/S)$	$\Delta G_{*H}(TM)$
Cr@N2B1-GDY	1.0555	-0.8521	-0.0046
Mn@N1B2-GDY	-0.5579	-0.8440	0.0467
Fe@N1S2-GDY	-	-	-0.0356
Co@N1B4-GDY	-1.2619	-0.3371	0.0353
Ni@N2-GDY	-0.0111		-0.0209

Table S7 The calculated adsorption free energies of the 5 promising systems under implicit solvation effects.

ΔG_{*H}	Without implicit solvation effect	With implicit solvation effect
Cr@N2B1-GDY	-0.0046	0.0369
Mn@N1B2-GDY	0.0467	0.9593
Fe@N1S2-GDY	-0.0356	0.0329
Co@N1B4-GDY	0.0353	-0.0864
Ni@N2-GDY	-0.0209	0.1393

Table. S8 Comparison of the adsorption energies (E_{ads}) and Gibbs free energies (ΔG_{*H}) between the 5 TM@HM-GDY candidates and their corresponding SAC-GDY systems.

	E_{ads}	ΔG_{*H}
Cr@N2B1-GDY	-0.2423	-0.0046
Cr-GDY	-4.0618	-3.8261
Mn@N1B2-GDY	-0.1305	0.0467
Mn-GDY	-14.1327	-13.9732
Fe@N1S2-GDY	-0.3066	-0.0356
Fe-GDY	-15.4884	-15.2480
Co@N1B4-GDY	-0.2451	0.0353
Co-GDY	-24.1867	-23.9120
Ni@N2-GDY	-0.2860	-0.0209
Ni-GDY	-16.3838	-16.1629

Table S9 The Bader charge of TM atom in 5 TM@NM-GDY catalysts.

	TM	*H
Cr@N2B1-GDY	-1.06	1.28
Mn@N1B2-GDY	-0.99	1.31
Fe@N1S2-GDY	-0.75	1.14
Co@N1B4-GDY	-0.63	1.05
Ni@N2-GDY	-0.52	1.17

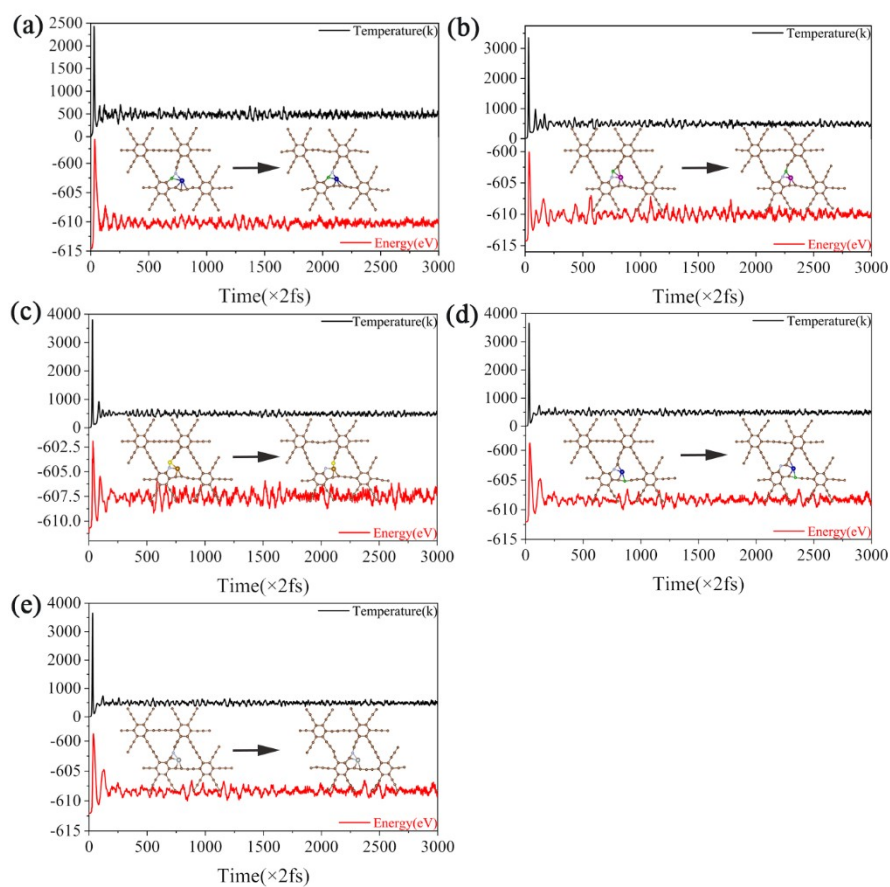


Fig. S1 The AIMD simulations of (a) Cr@N2B1-GDY, (b) Mn@N1B-GDY, (c) Fe@N1S2-GDY, (d) Co@N1B4-GDY and (e) Ni@N2-GDY.

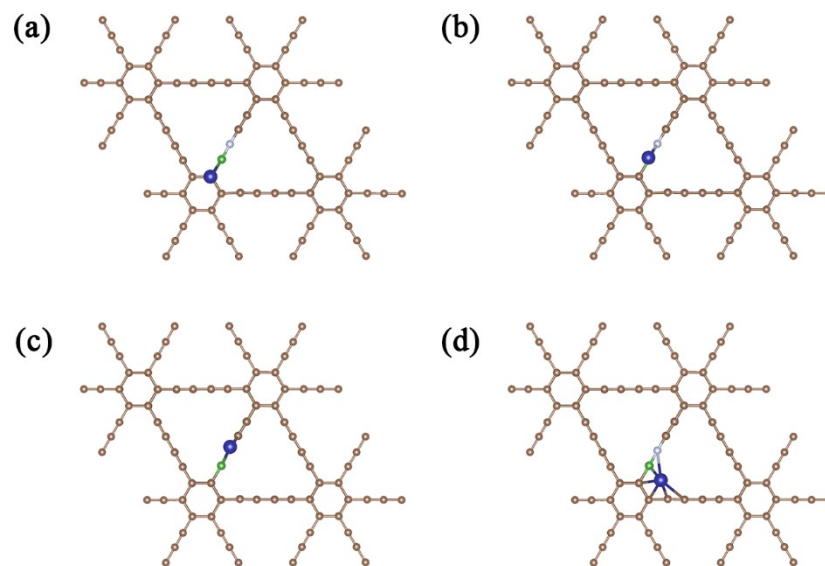


Fig. S2 Top view of the TM atom adsorption sites, taking the Cr@N2B1-GDY configuration as an example.

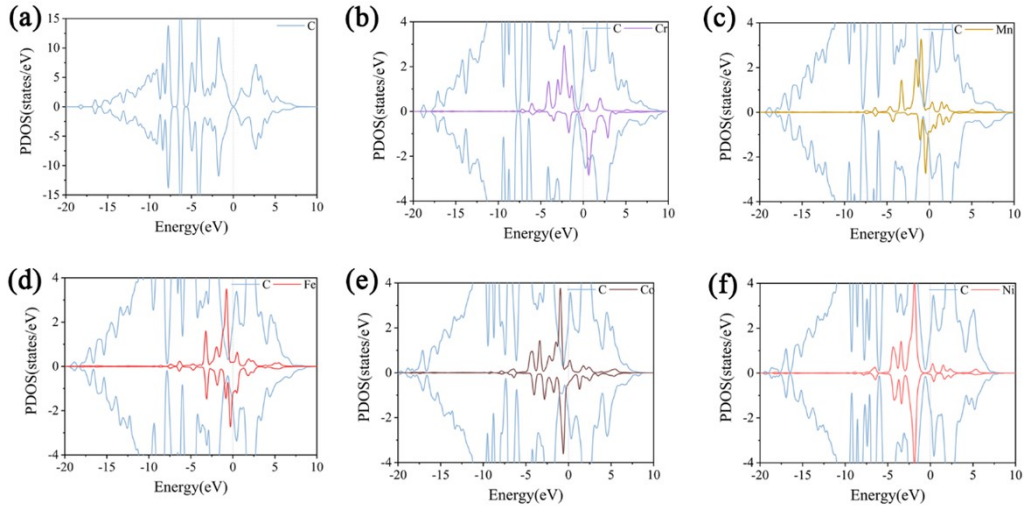


Fig. S3 The partial density of states (PDOS) of (a) pristine GDY, (b) Cr-GDY, (c) Mn-GDY, (d) Fe-GDY, (e) Co-GDY and (f) Ni-GDY.

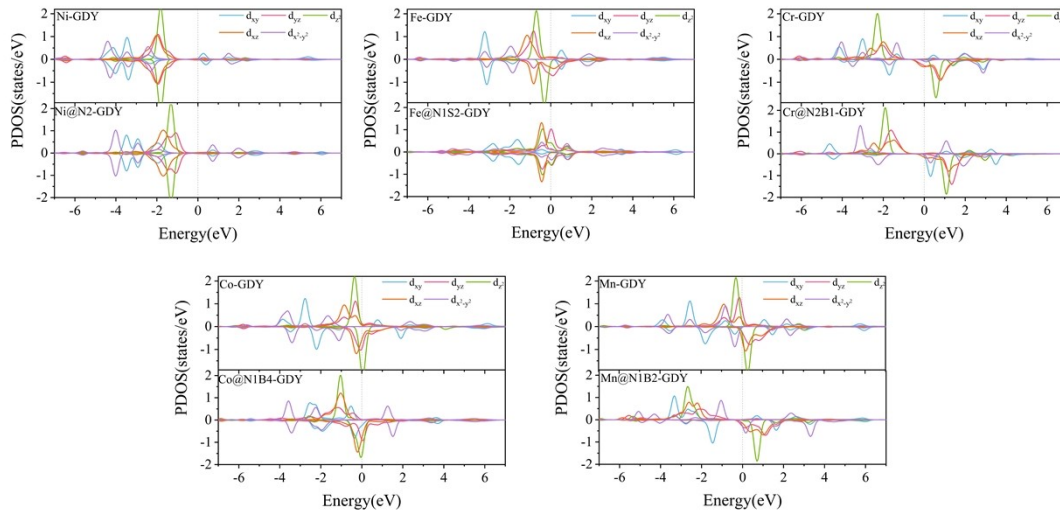


Fig. S4 The partial density of states (PDOS) of the TM center in SAC-GDY and TM@HM-GDY.

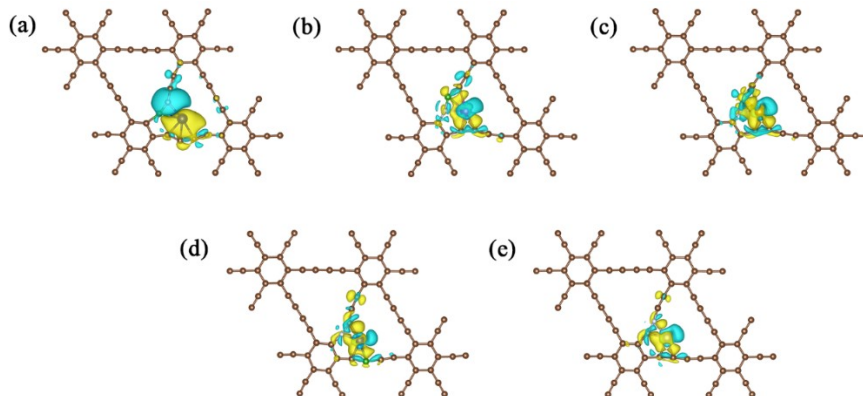


Fig. S5 Top views of the three-dimensional charge density difference plots for (a) Cr@N2B1-GDY, (b) Mn@N1B2-GDY, (c) Fe@N1S2-GDY, (d) Co@N1B4-GDY and (e) Ni@N2-GDY with an isovalue of $0.003 \text{ e } \text{\AA}^3$.

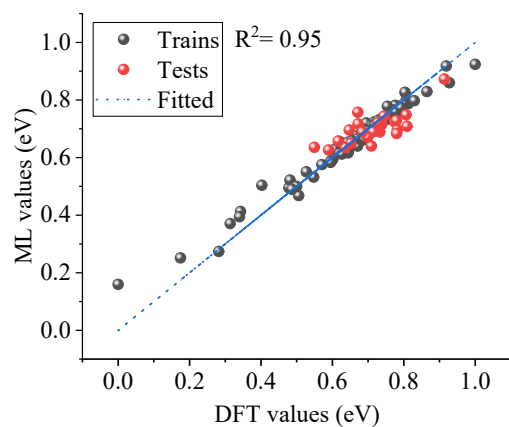


Fig. S6. Distribution of true and predicted values of RF machine learning model without principal component analysis

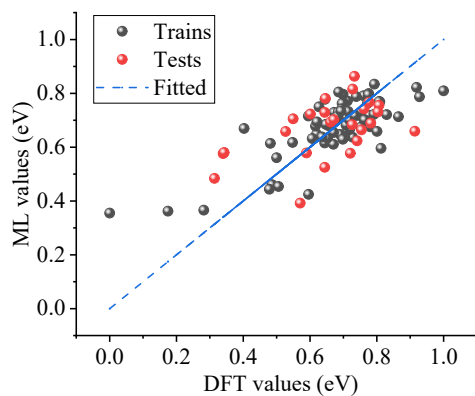


Fig. S7. Distribution of true and predicted values of ElasticNet machine learning model

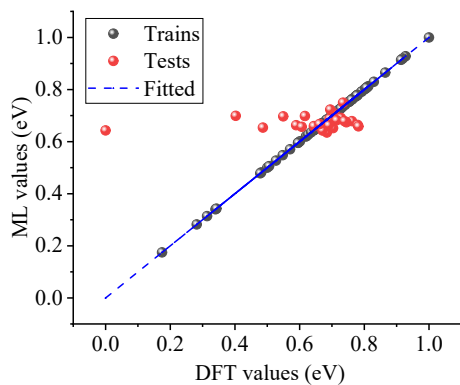


Fig. S8. Distribution of true and predicted values of KNN machine learning model

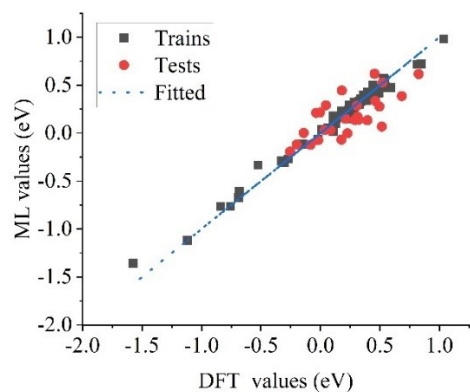


Fig. S9 True value and predicted value in MGBost machine learning model

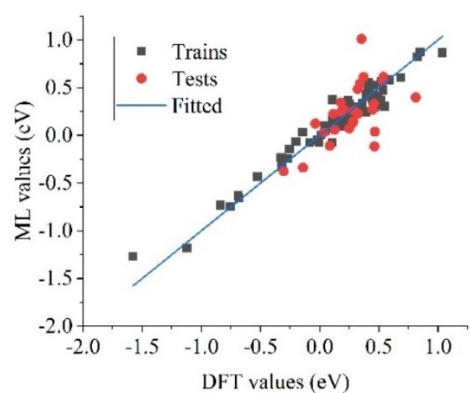


Fig. S10 True value and predicted value in LGB machine learning model

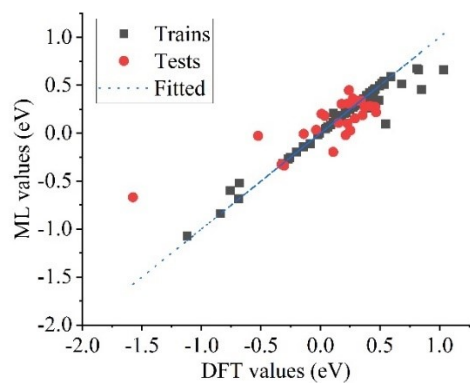


Fig. S11 True value and predicted value in SVR machine learning model